Electron Photodetachment from Organophosphide Ions. Electron Affinities and Substituent Effects in Organophosphines and Their Conjugate Radicals

Susan Berger and John I. Brauman*

Contribution from the Department of Chemistry, Stanford University, Stanford, California 94305-5080. *Received December 17, 1990. Revised Manuscript Received June 13, 1991*

Abstract: Electron photodetachment from methylphosphide, cyclohexylphosphide, and phenylphosphide ions was carried out using an ion cyclotron resonance (ICR) spectrometer to generate, trap, and detect the ions. The electron affinities of the corresponding radicals inferred from the onsets were as follows: methylphosphinyl, 21.6 ± 0.4 kcal/mol; cyclohexylphosphinyl, 23.8 ± 0.4 kcal/mol; and phenylphosphinyl, 35.1 ± 0.9 kcal/mol. The acidity of methylphosphine was determined by bracketing reactions to be ΔH°_{acid} between 371.5 and 366.4 kcal/mol, giving a P–H bond energy in methylphosphine between 74 and 79.5 kcal/mol.

Introduction

There have been numerous studies exploring the thermochemistry of first- and second-row main-group compounds including those of carbon,[1-3] nitrogen,[3-7] oxygen,[8-11] silicon,[12-16] phosphorus,[17-23] and sulfur.[9,11,24-27] However, among these main-group elements least is known about the thermochemistry of phosphorus compounds, despite the versatility and widespread use of organophosphorus compounds in such diverse applications as reagents in synthetic organic chemistry,[28] ligands in organotransition-metal complexes,[29] and pesticides and pharmaceuticals.[30] Most thermochemical studies have focused on phosphine, the simplest organophosphorus compound. Gas-phase ion studies have been used to determine the acidity[21,22] and bond dissociation energy[19,20] of PH_3, the basicity[31,32] of PH_2^-, and the electron affinity[17,18] of $PH_2^\bullet$. Thermochemical data on alkyl- and arylphosphides are less extensive. Ingemann and Nibbering[33] and Grabowski, Roy, and Leone[34] have independently measured the C–H gas-phase acidity of the methyl group in trimethylphosphine. In addition, theoretical investigations[35-37] have addressed the effect of alkyl substitution on the P–H acidity of phosphine.

In this paper we report the results of an investigation of the electron affinities of some organophosphinyl radicals and the acidity and thermochemistry of some organophosphines. We have used electron photodetachment spectroscopy to measure the electron affinities of methylphosphide, cyclohexylphosphide, and phenylphosphide radicals. Additionally, we have bracketed the P–H gas-phase acidity of methylphosphine using Fourier transform mass spectrometry and derived the P–H bond energy in methylphosphine. This study extends the existing thermochemical data for substituted hydrides of the first- and second-row main-group elements and allows us to examine several interesting trends in the electron affinities, bond dissociation energies, and acidities of these compounds.

Experimental Section

General. The study of organophosphide anions utilized an ion cyclotron resonance (ICR) spectrometer[38] to generate, trap, and detect the ion. Two types of experiments were performed using the ICR spectrometer: electron photodetachment[39] and acidity bracketing. In photodetachment experiments, the anion concentration, A^-, is monitored as a function of the wavelength (energy) of the irradiating light, eq 1.

(1) DePuy, C. H.; Gronert, S.; Barlow, S. E.; Bierbaum, V. M.; Damrauer, R. *J. Am. Chem. Soc.* **1989**, *111*, 1968.
(2) (a) Russell, J. J.; Seetula, J. A.; Timonen, R. S.; Gutman, D.; Nava, D. F. *J. Am. Chem. Soc.* **1988**, *110*, 3084. (b) Russell, J. J.; Seetula, J. A.; Gutman, D. *J. Am. Chem. Soc.* **1988**, *110*, 3092.
(3) Drzaic, P. S.; Brauman, J. I. *J. Phys. Chem.* **1984**, *88*, 5285.
(4) Smyth, K. C.; Brauman, J. I. *J. Chem. Phys.* **1972**, *56*, 4620.
(5) Mackay, G. I.; Hemsworth, R. S.; Bohme, D. K. *Can. J. Chem.* **1976**, *54*, 1624.
(6) Wickham-Jones, C. T.; Ervin, K. M.; Ellison, G. B.; Lineberger, W. C. *J. Chem. Phys.* **1989**, *91*, 2762.
(7) Brauman, J. I.; Blair, L. K. *J. Am. Chem. Soc.* **1971**, *93*, 3911.
(8) Schultz, P. A.; Mead, R. D.; Jones, P. L.; Lineberger, W. C. *J. Chem. Phys.* **1982**, *77*, 1153.
(9) Engelking, P. C.; Ellison, G. B.; Lineberger, W. C. *J. Chem. Phys.* **1978**, *69*, 1826.
(10) Janousek, B. K.; Zimmerman, A. H.; Reed, K. J.; Brauman, J. I. *J. Am. Chem. Soc.* **1978**, *100*, 6142.
(11) Richardson, J. H.; Stephenson, L. M.; Brauman, J. I. *J. Am. Chem. Soc.* **1975**, *97*, 2967.
(12) Walsh, R. In *The Chemistry of Organosilicon Compounds*; Patai, S., Rappoport, Z., Eds.; John Wiley & Sons: New York, 1989; Chapter 5.
(13) Wetzel, D. M.; Salomon, K. E.; Berger, S.; Brauman, J. I. *J. Am. Chem. Soc.* **1989**, *111*, 3835.
(14) Damrauer, R.; Kass, S. R.; DePuy, C. H. *Organometallics* **1988**, *7*, 637.
(15) Walsh, R. *Acc. Chem. Res.* **1981**, *14*, 246.
(16) Kanabus-Kaminska, J. M.; Hawari, J. A.; Griller, D.; Chatgilialoglu, C. *J. Am. Chem. Soc.* **1987**, *109*, 5267.
(17) Zittel, P. F.; Lineberger, W. C. *J. Chem. Phys.* **1976**, *65*, 1236.
(18) Smyth, K. C.; Brauman, J. I. *J. Chem. Phys.* **1972**, *56*, 1132.
(19) McAllister, T.; Lossing, F. P. *J. Phys. Chem.* **1969**, *73*, 2996.
(20) Berkowitz, J.; Curtiss, L. A.; Gibson, S. T.; Greene, J. P.; Hillhouse, G. L.; Pople, J. A. *J. Chem. Phys.* **1986**, *84*, 375.
(21) Bartmess, J. E.; Scott, J. A.; McIver, R. T., Jr. *J. Am. Chem. Soc.* **1979**, *101*, 6046.
(22) Brauman, J. I.; Eyler, J. R.; Blair, L. K.; White, M. J.; Comisarow, M. B.; Smyth, K. C. *J. Am. Chem. Soc.* **1971**, *93*, 6360.
(23) Holtz, D.; Beauchamp, J. L.; Eyler, J. R. *J. Am. Chem. Soc.* **1970**, *92*, 7045.
(24) Brauman, J. I.; Janousek, B. K. *Phys. Rev. A* **1981**, *23*, 1673.
(25) Brauman, J. I.; Janousek, B. K. *J. Chem. Phys.* **1980**, *72*, 694.
(26) Janousek, B. K.; Reed, K. J.; Brauman, J. I. *J. Am. Chem. Soc.* **1980**, *102*, 3125.
(27) Moran, S.; Ellison, G. B. *J. Phys. Chem.* **1988**, *92*, 1794.
(28) March, J. *Advanced Organic Chemistry*; McGraw Hill: New York, 1977; Chapter 16.
(29) Collman, J. P.; Hegedus, L. S. *Principles and Applications of Organotransition Metal Chemistry*; University Science: Mill Valley, CA, 1980; Chapter 3.
(30) (a) Emsley, J.; Hall, D. *The Chemistry of Phosphorus*; Harper & Row: New York, 1976. (b) Kosolapoff, G. M.; Maier, L. *Organic Phosphorus Compounds*; Wiley-Interscience: New York, 1972; Vol. 1. (c) Kirby, A. J.; Warren, S. G. *The Organic Chemistry of Phosphorus*; Elsevier: New York, 1967.
(31) Ikuta, S.; Kebarle, P. *Can. J. Chem.* **1983**, *61*, 97.
(32) Staley, R. H.; Beauchamp, J. L. *J. Am. Chem. Soc.* **1974**, *96*, 6252.
(33) Ingemann, S.; Nibbering, N. M. M. *J. Chem. Soc., Perkin Trans. 2* **1985**, 837.
(34) Grabowski, J. J.; Roy, R. D.; Leone, R. *J. Chem. Soc., Perkin Trans. 2* **1988**, 1627.
(35) Lohr, L. L.; Ponas, S. H. *J. Phys. Chem.* **1984**, *88*, 2992.
(36) Glidewell, C.; Thomson, C. *J. Comput. Chem.* **1982**, *3*, 495.
(37) Magnusson, E. *Aust. J. Chem.* **1985**, *38*, 23.
(38) A description of the ICR apparatus utilized in our laboratory for electron photodetachment studies may be found in the following: Wetzel, D. M.; Brauman, J. I. *Chem. Rev.* **1987**, *87*, 607.
(39) Relative cross sections were calculated from fractional signal decreases and power measurements using the steady-state model, as described in the following: Zimmerman, A. H. Ph.D. Thesis, Stanford University, 1977.

0002-7863/92/1514-4737$03.00/0

$$A^- + h\nu \rightarrow A + e^- \quad (1)$$

In the acidity-bracketing experiment, the acidity of the species of interest, HA, is determined by following the proton-transfer reaction between HA and the conjugate base, B^-, of a reference acid of known acidity, or its reverse, eq 2.

$$HA + B^- \rightleftharpoons A^- + HB \quad (2)$$

For a reference acid HB which is more acidic than HA, reaction 2 will not be observed in the forward direction. Similarly, for a reference acid less acidic than HA, the reverse reaction will not occur. In a bracketing experiment, the acidity of HA is bounded using two reference acids (and their conjugate bases), one of greater acidity and one of lesser acidity.

Materials. The neutral precursor nitrogen trifluoride was purchased from Ozark-Mahoning. The reference acid 2,2-difluoroethanol was obtained from Gallard Schlesinger Chemical Manufacturers. Cyclohexylphosphine and phenylphosphine were also available commercially (Strem Chemicals). Methylphosphine was synthesized by lithium aluminum hydride reduction of dimethyl methylphosphonate following the procedure described by Crosbie and Sheldrick.[40] Because of the pyrophosphoric nature of these organophosphines, samples were handled on a vacuum line or in a glovebag only. Before being admitted to the ICR cell, all compounds were subjected to several freeze–pump–thaw cycles to remove any volatile impurities.

Ion–Generation. The primary ion, F^-, was prepared via dissociative electron capture by nitrogen trifluoride, NF_3:

$$NF_3 + e^- \rightarrow F^- + NF_2 \quad (3)$$

The substituted phosphide anions were prepared by proton abstraction from the neutral organophosphines, eq 4–6:

$$MePH_2 + F^- \rightarrow MePH^- + HF \quad (4)$$

$$c\text{-}C_6H_{11}PH_2 + F^- \rightarrow c\text{-}C_6H_{11}PH^- + HF \quad (5)$$

$$C_6H_5PH_2 + F^- \rightarrow C_6H_5PH^- + HF \quad (6)$$

When the methylphosphide anion, $MePH^-$, was generated, an ion of m/z 33, presumably PH_2^-, was also formed.

The conjugate base of the reference acid 2,2-difluoroethanol (CF_2HCH_2OH) was also formed via proton abstraction by fluoride ion:

$$CF_2HCH_2OH + F^- \rightarrow CF_2HCH_2O^- + HF \quad (7)$$

The optimum conditions for formation of the organophosphide anions corresponded to a ratio of nitrogen trifluoride to neutral organophosphine of 1:3. Total pressures in the ICR cell were in the mid-10^{-7}-Torr range for photodetachment experiments and the low-10^{-6}-Torr region for acidity measurements, as determined with an uncalibrated ionization gauge (Varian, UHV-24).

Instrumental Procedures. A. ICR Apparatus. For photodetachment experiments, the ICR spectrometer was operated in the CW mode,[41] which allows continuous ion generation. The superior signal-to-noise of CW ICR allows measurement of small changes (ca. 0.5%) in the ion population. The ion detection circuitry consisted of a home-built capacitance bridge detector (CBD) circuit,[42,43] which utilized a commercial lock-in amplifier with a voltage-controlled oscillator (Princeton Applied Research Corp., Model 124A). A frequency-lock system[42b] was employed to correct for resonance frequency shifts (typically ±0.1 kHz in 150 kHz) which occur during photochemical experiments.

The acidity-bracketing experiments were accomplished using pulsed ICR spectrometry and a Fourier transform mass spectrometry (FTMS)[44] data collection system (IonSpec FTMS-2000). Double resonance techniques[45] permitted selective ejection of ions, allowing observation of the effect of a particular ion on the reaction of interest, uncomplicated by interfering species.

B. Light Sources. The light source was a 1000-W xenon arc lamp (Canrad-Hanovia), used with a 0.25-m high-intensity grating monochromator (Kratos Analytical), producing continuous radiation from approximately 250 to 1500 nm. Two gratings were employed: infrared (700–1500 nm) and visible (400–800 nm). Long-pass filters were used to block high-order light. The bandwidth of the light, determined by the slit width of the matching entrance and exit slits of the monochromator and the reciprocal linear dispersion of the diffraction grating, was 20 nm (ca. 0.4–0.9 kcal/mol, depending on wavelength region) at full-width half maximum (fwhm) in the threshold region of the spectra.

The output from the arc lamp in the regions of interest was monitored using a thermopile (Eppley Laboratory, Inc.). Because of the configuration of the experimental apparatus, the power measurements could not be taken concurrently with the ion signal measurements and, consequently, were taken immediately following ion signal measurements.

Calibration of the grating monochromater was accomplished using neon and mercury spectral lamps (Oriel Optics Corp.). Light from a tunable dye laser and a helium–neon laser was used to verify the calibration. The accuracy of the calibration was approximately ±2 nm (±0.03–0.08 kcal/mol, depending on wavelength). The uncertainty in the calibration of the light source did not make a significant contribution to the error in assigning the onset wavelength. Rather, the bandwidth of the light source, the energy separation of consecutive data points, and the signal-to-noise ratio in the threshold region were considered important in assessing the uncertainty in the onset assignment.

C. Data Acquisition and Processing. In the electron photodetachment experiment, the ion concentration (ion signal magnitude) was measured in the absence and presence of light as the wavelength was scanned. The probability for inducing electron loss from an anion is given by the relative cross section,[39] $\sigma(\lambda)$, which can be calculated from the fractional signal decrease, $F(\lambda)$, the wavelength, λ, and the energy of the light at wavelength λ, $E(\lambda)$:

$$\sigma(\lambda) = F(\lambda)/[\lambda E(\lambda)(1 - F(\lambda))] \quad (8)$$

Data acquisition and processing were accomplished using an IBM-XT computer to control the wavelength scanning, record ion signal and power measurements, calculate the relative cross sections, and average and splice cross-section files. The photodetachment spectra of the organophosphide anions comprise averaged data from several partially overlapping scan regions that were spliced together. The size of the scan region was dictated by the long-term stability of the ion signal, and scans were limited to between 10 and 15 min in duration. In this time span, base-line ion signal changes were usually less than 1%. Wavelength scans typically covered roughly 200 nm, with a spacing of approximately 5 nm (ca. 0.1–0.2 kcal/mol in the threshold region) between consecutive data points. The signal was allowed to equilibrate for roughly 10 s at each wavelength prior to data acquisition. Data at each wavelength were collected for approximately 3 s and represented an average of 10000 digitized points.

Results

Anionic Reaction Products. Reaction of fluoride ion with cyclohexylphosphine and phenylphosphine, eq 5 and 6, resulted solely in the formation of the proton abstraction products, cyclohexylphosphide and phenylphosphide anions, respectively. In generating the methylphosphide anion, however, two products were observed: $MePH^-$ (m/z 47) and PH_2^- (m/z 33). The methylphosphide anion is formed via proton abstraction from the parent compound by fluoride ion. We did see some small conversion of $MePH^-$ to PH_2^-, suggesting that PH_3 is present. The S_N2 displacement of F^- on $MePH_2$, giving MeF and PH_2^-, is probably endothermic. For this reaction to be exothermic, a C–P bond strength of less than 60 kcal/mol would be required, given the EAs of F and PH_2 and the C–F bond strength in MeF. Under conditions of the photodetachment experiments, $MePH^-$ was always present in greater quantities than PH_2^-. The ratio was roughly 3:2.

Identification of Regiochemistry of Ionic Products. The regiochemistry of the m/z 47 ion was ambiguous since proton abstraction could occur from either phosphorus or carbon. Our assignment of the m/z 47 ion as the methylphosphide anion, rather than the α-phosphinyl carbanion, is based on the experimental

(40) Crosbie, K. D.; Sheldrick, G. M. *J. Inorg. Nucl. Chem.* **1969**, *31*, 3684.

(41) Lehman, T. A.; Bursey, M. M. *Ion Cyclotron Resonance Spectrometry*; Wiley Interscience: New York, 1979; Chapter 1.

(42) (a) Original circuitry reported in the following: McIver, R. T., Jr.; Hunter, R. L.; Ledford, E. B., Jr.; Locke, M. J.; Francl, T. J. *Int. J. Mass Spectrom. Ion Phys.* **1981**, *39*, 65. (b) Implementation and modifications can be found in the following: Marks, J.; Drzaic, P. S.; Foster, R. F.; Wetzel, D. M.; Brauman, J. I.; Uppal, J. S.; Staley, R. H. *Rev. Sci. Instrum.* **1987**, *58*, 1460.

(43) Characteristics of the capacitance bridge detector indicating linear response with ion concentration may be found in the following: McIver, R. T., Jr.; Ledford, E. B., Jr.; Hunter, R. L. *J. Chem. Phys.* **1980**, *72*, 2535.

(44) For a detailed description of Fourier transform mass spectrometry, see: Freiser, B. S. In *Techniques for the Study of Ion-Molecule Reactions*: Farrar, J. M., Saunders, W. H., Jr., Eds.; John Wiley and Sons: New York, 1988; Chapter 3.

(45) Anders, L. R.; Beauchamp, J. L.; Dunbar, R. C.; Baldeschwieler, J. D. *J. Chem. Phys.* **1978**, *45*, 111.

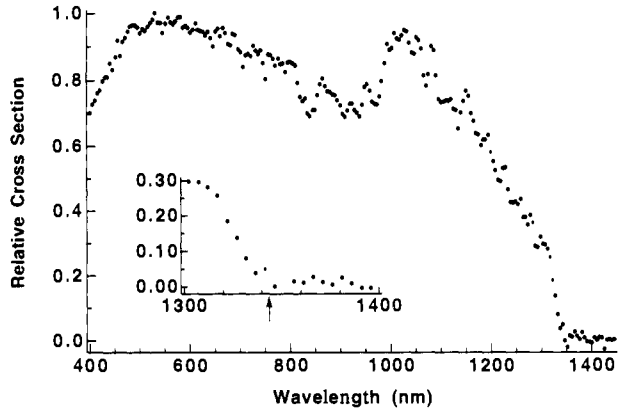

Figure 1. Photodetachment spectrum of methylphosphide anion. The arrow indicates the extrapolated onset. The bandwidth-corrected onset corresponds to 1322 ± 20 nm (21.6 ± 0.4 kcal/mol).

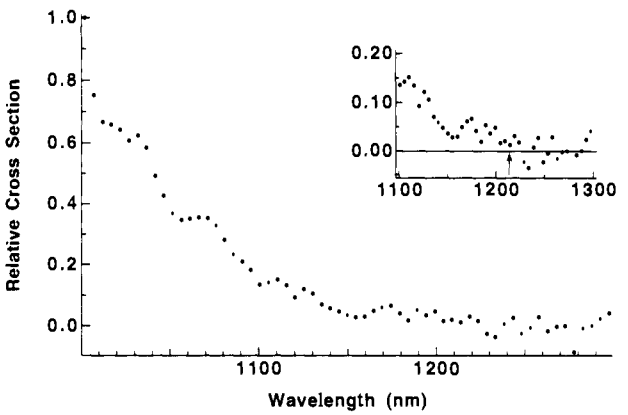

Figure 2. Photodetachment spectrum of cyclohexylphosphide anion. The arrow indicates the extrapolated onset. The bandwidth-corrected onset for photodetachment corresponds to 1202 ± 20 nm (23.8 ± 0.4 kcal/mol).

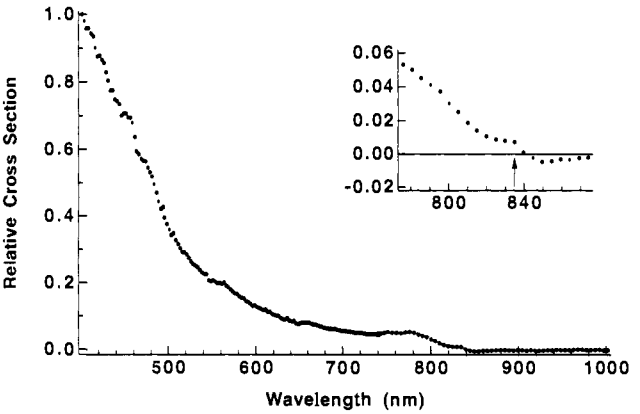

Figure 3. Photodetachment spectrum of phenylphosphide anion. The arrow indicates the extrapolated onset. The bandwidth-corrected onset corresponds to 815 ± 20 nm (35.1 ± 0.9 kcal/mol).

acidities for phosphine[46] and trimethylphosphine[33,34] ($\Delta H°_{acid}$-(PH_2–H) = 370.4 ± 2 kcal/mol and $\Delta H°_{acid}(Me_2PCH_2–H)$ = 391.3 ± 2 kcal/mol, or 384 ± 3 kcal/mol). The formation of the m/z 47 ion occurred via proton abstraction by fluoride ion, which is not nearly basic enough[46] ($\Delta H°_{acid}$(HF) = 371.0 ± 0.3 kcal/mol) to abstract a proton from carbon in the organophosphine. The acidities of the phosphines are consistent with calculations by Lohr and Ponas[35] which predict that the hydrogens on the phosphorus in $MePH_2$ are roughly 25 kcal/mol more acidic than those of the methyl group. Furthermore, the results of our acidity-bracketing experiments indicate that the m/z 47 ion has an acidity more consistent with the P–H acidity of phosphine than the C–H acidity of trimethylphosphine.

In order to demonstrate further the structure of the deprotonation product, we employed an extension of the N_2O reaction scheme devised by DePuy and co-workers.[47,48] The utility of this scheme is based on the observation that N_2O reacts with α-silyl carbanions and methylsilyl anions to yield products with different mass-to-charge ratios:

$$\underset{m/z\ \mathrm{M}}{R_2SiHCH_2^-} + N_2O \rightarrow \underset{m/z\ (\mathrm{M}+2)}{R_2SiHO^-} + CH_2N_2 \qquad (9)$$

$$\underset{m/z\ \mathrm{M}'}{R_3Si^-} + N_2O \rightarrow \underset{m/z\ (\mathrm{M}'+16)}{R_3SiO^-} + N_2 \qquad (10)$$

Thus, the regiochemistry of the (M − 1) species can be ascertained from the mass-to-charge ratio of the N_2O reaction product. Ingemann and Nibbering[33] and Grabowski and co-workers[34] have generated the (dimethylphosphinyl)methyl anion, $Me_2PCH_2^-$, by proton abstraction from trimethylphosphine by hydroxide ion. When the (dimethylphosphinyl)methyl anion was allowed to react with N_2O, a diazotization product was formed:

$$Me_2PCH_2^- + N_2O \rightarrow Me_2PCN_2^- + H_2O \qquad (11)$$

When we allowed the m/z 47 ion to react with N_2O and monitored the reaction using pulsed ICR and Fourier transform mass spectrometry, we observed the formation of an ion of m/z 63. This ion of m/z 63 was presumably $MePHO^-$, which would be consistent with the identification of the m/z 47 ion as the methylphosphide ion, in analogy to eq 10.

$$m/z\ 47 + N_2O \rightarrow Me_2PHO^- + N_2 \qquad (12)$$

If the m/z 47 ion was an α-phosphinyl carbanion, we expect that reaction with N_2O would yield either H_2PO^- (m/z 49) or $H_2PCN_2^-$ (m/z 73), or both, in analogy with eq 9 and 11. However, only a small amount of the m/z 49 ion was observed, which we attribute to the reaction of N_2O with PH_2^-, which could not be completely ejected from the ICR cell. We did not observe the m/z 73 ion.

Electron Photodetachment Spectra and Electron Affinities. The electron photodetachment spectra obtained for the methylphosphide, cyclohexylphosphide, and phenylphosphide anions are shown in Figures 1, 2, and 3. All three photodetachment spectra exhibit cross-section curves which are generally smooth in nature and are increasing functions of photon energy at threshold.

The cross section at a particular wavelength is the sum of all allowed transitions from the ground state of the anion to various rotational, vibrational, and electronic states of the radical. Transitions to excited electronic states of the anion or radical appear as additional onsets (slope changes) superimposed on the rising cross-section background. The onset, or threshold, for photodetachment is the wavelength (energy) at which the cross section first rises from 0. This onset is generally assigned as the adiabatic electron affinity of the radical, presuming that the Franck–Condon factors for the $v'' = 0 \leftarrow v' = 0$ transition are strong enough to be observed and that hot band transitions are unimportant.

From the photodetachment spectrum of methylphopshide anion, $MePH^-$ (Figure 1), the onset for the methylphosphide anion was determined using two methods. One method was a linear extrapolation of the data at threshold to zero cross section. The second method involved approximating the cross-section curve by a smoothed cubic spline[49] determined from a least-squares analysis.

(46) Lias, S. G.; Bartmess, J. E.; Liebman, J. F.; Holmes, J. L.; Levine, R. D.; Mallard, W. G. *J. Chem. Phys. Ref. Data* **1988**, *17*, (Suppl. 1).
(47) Bierbaum, V. M.; DePuy, C. H.; Shapiro, R. H. *J. Am. Chem. Soc.* **1977**, *99*, 5800.
(48) Damrauer, R.; DePuy, C. H. *Organometallics* **1984**, *3*, 362.
(49) For a discussion of the use of cubic spline functions and their derivatives in analyzing photodetachment spectra, see: (a) Janousek, B. K. Ph.D. Thesis, Stanford University, 1979, Chapter 2. (b) Janousek, B. K.; Zimmerman, A. H.; Reed, K. J.; Brauman, J. I. *J. Am. Chem. Soc.* **1978**, *100*, 6142 and reference 24 therein.

Table I. Electron Affinities of Organophosphide Radicals[a,b]

radical	EA (RPH)
HPH[c,d]	29.3 ± 0.2
MePH	21.6 ± 0.4
c-C_6H_{11}PH	23.8 ± 0.4
C_6H_5PH	35.1 ± 0.9

[a] Values in kcal/mol. [b] All values from this work unless otherwise noted. [c] Reference 17. [d] Reference 51.

The least-squares spline does not pass through all of the data points, but rather smooths the data by minimizing the difference between the data points and the smoothed spline function. The smoothed spline function was then differentiated to display slope changes in the cross-section curve. The extrapolation method and the differentiated spline method were in excellent agreement (values were within 2 nm (0.1 kcal/mol)), and the onset was assigned as 1342 ± 20 nm, based on the results from the differentiated spline method (arrow in Figure 1). To correct for the bandwidth of the monochromator (20 nm fwhm), the fwhm bandwidth was subtracted[50] from the observed onset, yielding a bandwidth-corrected onset of 1322 ± 20 nm. The electron affinity of the methylphosphide radical was assigned from the bandwidth-corrected onset as 21.6 ± 0.4 kcal/mol. The photodetachment spectrum for methylphosphide anion rises very sharply in the threshold region and reaches a plateau approximately 300 nm (0.26 eV) above threshold. In some regions of the methylphosphide photodetachment spectrum, particularly at 900–1200 nm, power spikes in the arc lamp output and the instability of the ion signal at these wavelengths make the data particularly noisy. The dips and peaks apparent in the cross section in these regions were not reproducible from run to run and have no physical significance.

Figure 2 shows the photodetachment spectrum obtained for the cyclohexylphosphide ion, c-$C_6H_{11}PH^-$. The photodetachment onset was obtained using a linear extrapolation of the data to zero cross section and a differentiated smoothed spline function, as described above. The values generated using these two methods were within 7 nm (0.1 kcal/mol) of each other. The onset was ultimately assigned on the basis of the differentiated spline method, yielding an onset of 1222 ± 20 nm (arrow in Figure 2). After correction for the monochromator bandwidth (20 nm fwhm), the onset was assigned as 1202 ± 20 nm, corresponding to an electron affinity of 23.8 ± 0.4 kcal/mol. The cross-section curve for the cyclohexylphosphide anion rises slowly in the threshold region, in contrast to the sharply rising curve exhibited by the methylphosphide anion. The observed changes in the threshold region were completely reproducible; the measurement of the cross section at shorter wavelength, however, was rather noisy, because the xenon lamp output has a spiky wavelength dependence in this region. Consequently, we have not presented the data from the higher-energy regime.

The electron photodetachment spectrum for phenylphosphide ion is shown in Figure 3. The onset for photodetachment was determined from the linear extrapolation and differentiated spline methods. The onsets extracted using these two analyses were within 5 nm (0.2 kcal/mol). The results from the latter method yielded an onset of 835 ± 20 nm (arrow in Figure 3). The bandwidth-corrected onset for phenylphosphide anion was assigned as 815 ± 20 nm, resulting in an electron affinity of 35.1 ± 0.9 kcal/mol for the phenylphosphide radical. The cross-section curve for phenylphosphide anion, in contrast to that of the methylphosphide anion, is slowly rising in the threshold region. Also, in contrast to the methylphosphide photodetachment spectrum, the phenylphosphide spectrum does not exhibit a plateau, but is strictly an increasing function of photon energy.

The results of our electron affinity measurements for methylphosphide, cyclohexylphosphide, and phenylphosphide radicals are summarized in Table I. The electron affinity of phosphide radical is included for comparison.

Table II. Electron Affinities of First- and Second-Row Main-Group Hydrides and Methyl-Substituted Hydrides[a]

CH_3	1.8 ± 0.7[b]	NH_2	17.8 ± 0.1[d]	OH	41.1 ± 0.1[f]
$MeCH_2$	−6.4 ± 1.0[c]	MeNH	13.1 ± 3.51[e]	MeO	36.2 ± 0.5[g]
SiH_3	32.4 ± 0.3[h]	PH_2	29.3 ± 0.2[j]	SH	53.4 ± 0.1[l]
$MeSiH_2$	27.5 ± 0.8[i]	MePH	21.6 ± 0.4[k]	MeS	43.2 ± 0.25[m]

[a] All values in kcal/mol. [b] Reference 54. [c] Reference 1. [d] Reference 6. See also ref 4. [e] Reference 5. [f] Reference 8. [g] Reference 9. See also ref 10. [h] Reference 55. See also ref 13. [i] Reference 13. [j] Reference 17. See also ref 18. [k] This work. [l] Reference 24. [m] Reference 27. See also refs 9, 25, and 26.

Replacement of hydrogen by a methyl group in the phosphide radical lowers the electron affinity by almost 8 kcal/mol. Replacement of hydrogen by a cyclohexyl group also causes a decrease in the electron affinity of the phosphide radical, although smaller, roughly 6 kcal/mol. In contrast to the effect of alkyl substitution, substitution of a hydrogen by a phenyl group raises the electron affinity of the phosphide radical by approximately 6 kcal/mol.

Acidity-Bracketing Experiments and the Gas-Phase Acidity. $MePH_2$ reacts with F^- to give the proton transfer product, $MePH^-$, eq 13. In the reaction of $MePH_2$, CF_2HCH_2OH, and their

$$F^- + MePH_2 \rightarrow HF + MePH^- \quad (13)$$

conjugate bases, only proton transfer from CF_2HCH_2OH to $MePH^-$ was observed, eq 14.

$$CF_2HCH_2OH + MePH^- \rightleftharpoons CF_2HCH_2O^- + MePH_2 \quad (14)$$

We also observed that $MePH^-$ would deprotonate methyl vinyl ketone and acetaldehyde, both of which are slightly more acidic than CF_2HCH_2OH. In addition, we were able to observe a small conversion of $MePH^-$ to PH_2^-, suggesting that $MePH_2$ and PH_3 have comparable acidities. The presence of phosphine in the methylphosphine sample should not have any effect in the conclusions drawn from these bracketing reactions. From these reactions, it was determined that methylphosphide is more acidic than[46] HF ($\Delta H°_{acid}(HF)$ = 371.0 ± 0.3 kcal/mol), but is less acidic than[46] CF_2HCH_2OH ($\Delta H°_{acid}(CF_2HCH_2OH)$ = 366.4 ± 2.9 kcal/mol). The acidity of methylphosphine was thus assigned as lying between the 366.4 ± 2.9 kcal/mol and 371.0 ± 0.3 kcal/mol. Proton-transfer equilibria are controlled by free energy rather than enthalpy changes. The reference acids used here have entropies of dissociation which differ from that of $MePH_2$ due to the number of acidic protons and changes in rotational entropy. Nevertheless, the energy spacing of the reference acids allows only for relatively crude bracketing, and we have used the *energy* requirement $\Delta H° \leq 0$ for reaction to occur.

Comparison of our bracketed acidity of methylphosphine with the measured acidity for phosphine[46] ($\Delta H°_{acid}(PH_3)$ = 370.9 ± 2.0 kcal/mol) reveals that methylphosphine is comparable in acidity to phosphine. This result is in contrast to theoretical work[35-37] which predicts that methylphosphine is roughly 7 kcal/mol less acidic than phosphine. If that were true, then F^- would not be capable of deprotonating $MePH_2$.

Derivation of Bond Dissociation Energies. The hydride homolytic bond dissociation energy, $D°(R–H)$, can be derived via a thermochemical cycle[52] using the electron affinity of the radical, $EA(R^•)$; the hydride gas-phase acidity, $\Delta H°_{acid}(R–H)$; and the ionization potential of hydrogen, $IP(H^•)$:

$$D°(R–H) = \Delta H°_{acid}(R–H) + EA(R^•) - IP(H^•) \quad (15)$$

We employed this thermochemical cycle to extract the bracketed P–H bond dissociation energy in methylphosphine using our bracketed P–H acidity of 366.4 ± 2.9 kcal/mol to 371.0 ± 0.3 kcal/mol for methylphosphine; our measured electron affinity of 21.6 ± 0.4 kcal/mol, for methylphosphide radical; and the ionization potential[53] of H•, 313.6 kcal/mol. Our derived P–H

(50) Smyth, K. C. Ph.D. Thesis, Stanford University, 1972, Chapter 3.
(51) Zittel and Lineberger's electron affinity measurement is consistent with the low-resolution determination of 28.8 + 0.7 kcal/mol. See ref 18.
(52) Drzaic, P. S.; Marks, J.; Brauman, J. I. In *Gas Phase Ion Chemistry*; Bowers, M. T., Ed.; Academic Press: Orlando, FL, 1984; Vol. 3.

Table III. Bond Dissociation Energies [$D°$(R–H)] of First- and Second-Row Main-Group Hydrides and Methyl-Substituted Hydrides[a]

CH_3–H	104.8 ± 1.0[b]	NH_2–H	107.4 ± 1.1[c]	OH–H	119[e]
$MeCH_2$–H	100.1 ± 1.0[b]	MeNH–H	100.0 ± 2.5[d]	MeO–H	104.4 ± 1.0[f]
SiH_3–H	91.6 ± 2[g]	PH_2–H	83.9 ± 3[h]	SH–H	91.1 ± 0.2[c]
$MeSiH_2$–H	92.2 ± 3[g]	MePH–H	74.4–79.0[i]	MeS–H	87.0 ± 2.2[j]

[a] All values in kcal/mol. [b] Reference 1. [c] Reference 61. [d] Reference 62. [e] Reference 63. [f] Reference 64. [g] Reference 13. See also ref 15. [h] Reference 19. See also ref 20. [i] This work. [j] Reference 65.

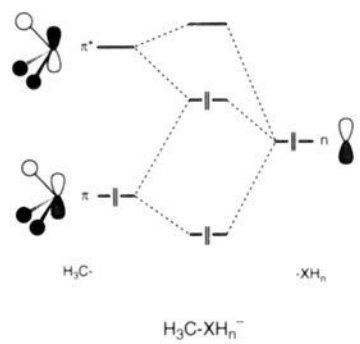

Figure 4. Schematic molecular orbital diagram of hyperconjugative interactions with a methyl substituent. In the neutral radical only three electrons are involved, so the HOMO would be singly occupied.

bond dissociation energy in methylphosphine lies between 74.4 ± 3.0 kcal/mol and 79.0 ± 0.6 kcal/mol.

Discussion

Alkyl Substitution and Electron Affinities. Electron affinities for the first- and second-row main-group radicals and methyl-substituted radicals are shown in Table II. Replacement of a hydrogen by a methyl group always lowers the electron affinity. The magnitude of this effect is similar for all the first- and second-row radicals: the electron affinity is lowered by approximately 5–10 kcal/mol upon replacement of a hydrogen by a methyl group.

The observed decrease in the electron affinity could be a consequence of destabilization of the anion upon methyl substitution, as proposed for the decreased electron affinities of methoxyl,[10] methylsilyl,[13,14] thiomethoxyl,[26,27] and ethyl.[1] Theoretical studies[56] predict that replacement of a hydrogen by a methyl group lowers the stability of both silyl and alkyl anions, relative to the corresponding parent neutral acids. The inductive effect of a methyl group destabilizes the anionic center by electron release through the σ framework, as suggested by Moran and Ellison[27] for thiomethoxide. Ab initio studies by Schleyer et al.[57] using (3-21+G) diffuse functions indicate that first-row elements can destabilize anions through inductive effects. Anion destabilization can also occur through hyperconjugative interactions.[58] Figure 4 shows a schematic molecular orbital diagram for the interaction of a methyl group fragment with a XH_n fragment. In the case of the anion, this is a four-electron interaction and is net destabilizing. Hyperconjugative interactions of the type shown in Figure 4 have been proposed to account for the decreased stability of methyl-substituted main-group hydride anions, such as oxygen-,[10] silicon-,[13] and sulfur-centered[26] anions.

In addition to destabilization of the anion, stabilization of the radical upon methyl substitution by inductive effects and hyperconjugation can also contribute to the lowering of the electron affinity, as discussed by DePuy and co-workers for the electron affinities of alkyl radicals,[1] and by Brauman et al. in studies of alkoxides[10] and mercaptides.[26] Hyperconjugation[58] in the radical involves only three electrons (Figure 4), and the interaction is stabilizing. Thus, destabilizing hyperconjugative interactions in the anion and stabilizing hyperconjugative interactions in the radical may contribute in varying degrees to the observed lowering of the electron affinity upon methyl substitution in main-group hydrides. In light of the varying magnitude of these factors, it is interesting that the size of this effect is so similar among these species.

A second trend is that the electron affinities for both hydrides and the methyl-substituted hydrides are always greater for the second-row species relative to the first-row. The larger size of the valence orbitals of the second-row species compared to those of the first-row species results in diminished electron repulsion with the core electrons, so that these anions are stabilized relative to their first-row counterparts and have a larger electron affinity. Moran and Ellison[27] comment on this in explaining the higher electron affinity of HS$^\bullet$ compared to HO$^\bullet$. In addition, the enhanced polarizability of the second-row species allows them to accommodate charge better, relative to the first-row species. The larger size and greater polarizability of the second-row species also result in a reduced electron repulsion among the valence electrons. In the case of carbon and silicon, hybridization diferences may also contribute to the larger electron affinity of the second-row species. In the methyl anion, the nonbonding electrons are in an orbital of almost pure p character. In contrast, the nonbonding electrons in silicon are in an orbital with substantial s character and are therefore held more tightly. This is evidenced by examining the H–Si–H bond angles of the silyl anion, which have been calculated[59] to be 97°. Since the nonbonding electrons are held more tightly in silyl anions, these anions are more stable relative to the carbanions.[13,60]

A third trend in Table II is that the electron affinities increase in going across a row both for the hydrides and for the methyl hydrides.[22] The electron affinities (and electronegativities) increase, in part, because of increasing nuclear charge which is not fully screened. The only exception to this trend occurs with silicon, which appears to have an anomalously high electron affinity. In the silyl anion, the increased s character of the nonbonding orbital causes the "extra" electron to be held more tightly compared with those anions in which the nonbonding electrons are in an orbital with primarily (or exclusively, for symmetry reasons) p character[13,36] (see above). In addition, silicon is unusual because its electronegativity is lower than that of hydrogen. In this case, we might expect the Si–H bonds to be polarized away from silicon, thereby allowing silicon to diffuse the negative charge in the anion by donation to the hydrogens, which would stabilize the silicon anion relative to the radical.

Alkyl Substitution and Bond Dissociation Energies. Table III presents the bond dissociation energies ($D°$(R–H)) for the first- and second-row main-group hydrides and methyl-substituted hydrides.

Substitution of a methyl group for hydrogen lowers the X–H bond dissociation energy in all the first- and second-row hydrides except silicon, which has an X–H bond energy unaffected by the

(53) Stull, D. R.; Prophet, H., Eds. *JANAF Thermochemical Table; National Standard Reference Data Series, National Bureau of Standards*; NSRDS-NBS 37; U.S. Government Printing Office: Washington, DC, 1971.
(54) Ellison, G. B.; Engelking, P. C.; Lineberger, W. C. *J. Am. Chem. Soc.* **1978**, *100*, 2556.
(55) Nimlos, M. R.; Ellison, G. B. *J. Am. Chem. Soc.* **1986**, *108*, 6522.
(56) Hopkinson, A. C.; Lien, M. H. *J. Org. Chem.* **1981**, *46*, 998.
(57) Spitznagel, G. W.; Clark, T.; Chandrasekhar, J.; Schleyer, P. v. R. *J. Comput. Chem.* **1982**, *3*, 363.
(58) For a description of anion destabilization and radical stabilization by hyperconjugation, see: Schleyer, P. v. R.; Kos, A. J. *Tetrahedron* **1983**, *39*, 1141.
(59) Eades, R. A.; Dixon, D. A. *J. Chem. Phys.* **1980**, *72*, 3309.
(60) Reed, K. J.; Brauman, J. I. *J. Chem. Phys.* **1974**, *61*, 4830.
(61) DeFrees, D. J.; Hehre, W. J.; McIver, R. T., Jr.; McDaniel, D. H. *J. Phys. Chem.* **1979**, *83*, 232.
(62) Golden, D. M.; Solly, R. K.; Gac, N. A.; Benson, S. W. *J. Am. Chem. Soc.* **1972**, *94*, 363.
(63) Lias, S. G.; Bartmess, J. E.; Liebman, J. F.; Holmes, J. L.; Levin, R. D.; Mallard, W. G. *J. Phys. Chem. Ref. Data* **1988**, *17* (Suppl. 1).
(64) Batt, L.; Christie, K.; Milne, R. T.; Summers, A. J. *Int. J. Chem. Kinet.* **1974**, *6*, 877.
(65) Shum, L. G. S.; Benson, S. W. *Int. J. Chem. Kinet.* **1983**, *15*, 433.

Table IV. Gas-Phase Acidities [$\Delta H°_{acid}$(R–H)] of First- and Second-Row Main-Group Hydrides and Methyl-Substituted Hydrides[a]

CH_3–H	416.6 ± 1.0[b]	NH_2–H	403.6 ± 0.8[c]	OH–H	390.7 ± 0.1[d]
$MeCH_2$–H	420.1 ± 1.0[b]	MeNH–H	403.2 ± 1.2[c]	MeO–H	380.6 ± 2.1[d]
SiH_3–H	372.8 ± 2[e]	PH_2–H	370.9 ± 2.0[g]	SH–H	351.2 ± 2.1[d]
$MeSiH_2$–H	378.3 ± 2[f]	MePH–H	364.4–371.5[h]	MeS–H	356.9 ± 2.9[d]

[a] All values in kcal/mol. [b] Reference 1. [c] Reference 5. [d] Reference 46. [e] Reference 13. See also refs 46 and 55. [f] Reference 13. [g] Reference 63. See also refs 22 and 23. [h] This work.

introduction of a methyl substituent. The lower bond dissociation energy suggests that methyl substitution stabilizes the radicals. The stabilizing effect of alkyl groups on radicals has been proposed for carbon- and sulfur-centered radicals[1,26,66,67] and includes inductive effects and hyperconjugative interactions, as discussed previously. The inductive effect results from electron release from the alkyl group, which stabilizes the electron-deficient radical moiety.[27]

A second feature in Table III is that the bond energies in both the hydrides and methyl hydrides are always lower in the second-row species relative to their first-row counterparts. Second-row species are larger than their first-row congeners and thus have poorer overlap with the hydrogen 1s orbital. In addition, the bond energies in the second-row compounds are lowered because of the diminished electronegativity of the second-row elements compared to the first-row elements. In general, the elements of the second row have electronegativities which are closer than those of the first-row species to the electronegativity of hydrogen. Consequently, the X–H bonds in the second-row compounds have a diminished polar contribution compared to those in the first-row. Since bond polarity increases the bond strength,[68] the diminished ionic contribution in second-row hydrides lowers the bond strength. Schleyer and co-workers[69] have used ab initio methods to show a strong correlation in silicon compounds between the strength of the bond and the electronegativity of the substituent: stronger bonds form with more electronegative substituent groups. The connection between these two properties has been attributed to the greater contributions from ionic structures of bonds to electronegative groups, as suggested long ago by Pauling.

Alkyl Substitution and Gas-Phase Acidities. The heterolytic enthalpies of dissociation, or gas-phase acidities, of the first- and second-row main-group hydrides and methyl hydrides are shown in Table IV.

The first trend evident in the hydride acidities is that the acidity is enhanced proceeding across a row. This effect is due to the increasing electron affinities. Although the bond dissociation energies also increase (which decreases the acidity), the changes are not as great as the changes in the electron affinities[22] and thus do not dominate the trend.

Second, both X–H and methyl-substituted X–H second-row species are always more acidic than their first-row counterparts. The enhanced acidity of the second-row hydrides relative to the first-row hydrides is mostly a consequence of the lower bond energies,[22] which in turn are a consequence of the poorer overlap involving the second-row heteroatom orbital (see above).

No obvious trend in the hydride acidities is apparent upon replacement of a hydrogen by a methyl group. In the first row, the acidity decreases in methane with methyl substitution, remains unchanged in ammonia, and increases in water. In the second row, methyl substitution diminishes the acidity of silane and hydrogen sulfide. The acidity of methylphosphine is, within the bracketing limits, indistinguishable from that of phosphine. Thus, substitution of a methyl group for a hydrogen can either enhance or diminish the X–H acidity. This behavior of the acidity upon methyl substitution can be understood by viewing the acidity in terms of other relevant thermochemical parameters: the electron affinity and the bond dissociation energy. These three thermochemical quantities are related via the thermochemical cycle, eq 15. A smaller bond energy or a higher electron affinity enhances the acidity. In the case of these hydrides, methyl substitution lowers the electron affinity by 5–10 kcal/mol (which has the effect of diminishing the acidity) and lowers the bond dissociation energy by 0–20 kcal/mol (which enhances the acidity). Since these two effects have opposing influences, the change in the acidity is not predictable a priori.

Table V. Electron Affinities of First- and Second-Row Main-Group Hydrides and Phenyl-Substituted Hydrides[a]

CH_3	1.8 ± 0.7[b]	NH_2	17.8 ± 0.1[d]	OH	41.1 ± 0.1[e]
$PhCH_2$	19.9 ± 0.3[c]	PhNH	39.3 ± 0.7[c]	PhO	52.4 ± 0.9[f]
SiH_3	32.4 ± 0.3[g]	PH_2	29.3 ± 0.2[i]	SH	53.4 ± 0.1[k]
$PhSiH_2$	33.1 ± 0.1[h]	PhPH	35.1 ± 0.9[j]	PhS	<57.0 ± 1.4[l]

[a] All values in kcal/mol. [b] Reference 54. [c] Reference 3. [d] Reference 6. See also ref 4. [e] Reference 8. [f] Reference 70. [g] Reference 55. See also ref 13. [h] Reference 13. [i] Reference 17. See also ref 18. [j] This work. [k] Reference 24. [l] Reference 11.

Aryl Substitution and Electron Affinities. Table V summarizes the electron affinities of the first- and second-row main-group binary hydrides and phenyl-substituted hydrides.

Replacement of a hydrogen by a phenyl group raises the electron affinity, in contrast to the effect of methyl substitution. The magnitude of the increase in the electron affinity by phenyl substitution varies from less than 1 kcal/mol to more than 20 kcal/mol. Phenyl substitution can stabilize the radical by delocalization of the unpaired electron into the phenyl ring,[15] an effect which would decrease the electron affinity. The electron affinity can be increased, however, by stabilization of the anion by the phenyl substituent. The phenyl group can stabilize an anion both inductively and conjugatively, although the former mechanism appears to be less important.[11,67,71] Delocalization of the nonbonding electrons is believed to occur in phenoxide anion (PhO^-),[11] thiophenoxide anion (PhS^-),[11] anilide anion ($PhNH^-$),[3] and benzyl anion ($PhCH_2^-$).[3] In contrast, the phenylsilyl anion ($PhSiH_2^-$) shows very little, if any, delocalization.[13,15]

Theoretical evidence has been provided for moderate conjugation between the phosphorus atom and the phenyl ring in phenylphosphide anion. Magnusson's[72] ab initio calculations using extended basis sets indicate that phenyl substituents gain electronic charge from phosphorus by conjugative transfer. Calculated bond orders[72] show an increased π-bond character upon deprotonation of phenylphosphine. NMR studies of compounds of the form RPH^- indicate a moderate phosphorus–ring conjugation.[73,74] Batchelor and Birchall[73] found evidence for considerable resonance delocalization in aniline ($PhNH_2$) and diphenylamine (Ph_2NH), but no similar effect in the neutral phosphorus congeners. Thus, in phenylphosphines considerable resonance delocalization occurs in the anions but is absent in the neutral parent conjugate acids.

A second trend in Table V is that the effect of phenyl substitution is much more pronounced in the case of the first-row species compared to the second-row species: the electron affinities of the first-row species are raised by roughly 10–20 kcal/mol by phenyl substitution, while in the corresponding second-row species

(66) Luria, M.; Benson, S. W. *J. Am. Chem. Soc.* **1975**, *97*, 3342.
(67) March, J. *Advanced Organic Chemistry*; Wiley and Sons: New York, 1985; Chapter 5.
(68) Sanderson, R. T. *Polar Covalence*; Academic Press: New York, 1983; Chapter 3.
(69) Luke, B. T.; Pople, J. A.; Krogh-Jespersen, M.; Apeloig, Y.; Chandrasekhar, J.; Schleyer, P. v. R. *J. Am. Chem. Soc.* **1986**, *108*, 260.
(70) Leopold, D. G.; Murray, K. K.; Lineberger, W. C. In *Experimentally Determined Electron Affinities*; Travers, M. J., Ellison, G. B., Eds.; University of Colorado: Boulder, CO, 1989.
(71) Jolly, W. H. *Inorg. Chem.* **1971**, *10*, 2364.
(72) Magnusson, E. *Phosphorus Sulfur* **1986**, *28*, 379.
(73) Batchelor, B.; Birchall, T. *J. Am. Chem. Soc.* **1982**, *104*, 674.
(74) Grim, S. O.; Molenda, R. P. *Phosphorus Relat. Group V Elem.* **1974**, *4*, 189.

the electron affinities are raised roughly from 1 to 6 kcal/mol. As perturbation arguments suggest, and as found in many other cases, increased stability (of the second-row anions) makes additional stabilization less important. The diminished phenyl-substituent effect in the second-row species relative to the first-row species is also a consequence of the weaker interaction with the phenyl group which arises from the poor overlap of the 3p orbitals of the second-row elements with the 2p orbitals of the ring. The large differences in the effect of phenyl substitution in carbanions vs silyl anions has been attributed[13] to energy mismatch and differences in orbital size, both of which contribute to less stabilization.

Conclusions

We have measured the electron affinities of alkyl- and aryl-substituted phosphide radicals. We have also bracketed the P–H acidity and derived the bracketed P–H bond energy for methylphosphine. Our data extend the existing thermochemical literature addressing substituent effects in the first- and second-row main-group hydrides. We find that replacement of a hydrogen by a methyl group always lowers the electron affinity of the hydride radical by 5–10 kcal/mol; that the hydride bond energies are always lowered upon methyl substitution, except in the case of silane (which remains unaffected); and that the second-row species are always more acidic than their first-row counterparts.

Acknowledgment. We are grateful to the National Science Foundation for support of this work. We thank E. Brinkman for helpful discussions.

Registry No. MePH, 109527-93-7; c-$C_6H_{11}PH$, 140149-12-8; PhPH, 17062-94-1; $MePH_2$, 593-54-4.

Theoretical Study of the Low-Lying Triplet and Singlet States of Diradicals. 1. Tetramethyleneethane

Petr Nachtigall and Kenneth D. Jordan*

Contribution from the Department of Chemistry, University of Pittsburgh, Pittsburgh, Pennsylvania 15260. *Received June 17, 1991*

Abstract: The geometry of the lowest energy singlet and triplet states of tetramethyleneethane have been optimized by means of the UHF, ROHF, and MCSCF methods, in order to obtain a better understanding of the importance of electron correlation for the geometries and the singlet–triplet gap. At the MCSCF(6,6)/DZP level of theory, both the singlet and triplet states are predicted to have D_2 structures, with the ground state being the singlet and the triplet state lying 1.36 kcal/mol higher in energy.

I. Introduction

The energy separation between the lowest singlet and triplet states of diradical species is a subject of considerable interest. One of the most studied diradicals is tetramethyleneethane (TME).[1-6] The two frontier orbitals (HOMO and LUMO) of TME are degenerate in the Hückel MO approximation. One triplet and three singlet states result from the various possible ways of distributing the two "frontier" electrons in these two orbitals. Of these four states, the two lowest in energy—the triplet state and one of the singlet states—are diradical in character.[1] The most sophisticated ab initio calculations carried out to date on TME predict a singlet ground state, lying energetically about 1.5 kcal/mol below the triplet state.[2] On the other hand, an ESR spectrum determined from the photodecomposition products of an azo precursor has been attributed to the triplet state of TME,[3] which would seem to imply either that TME has a ground-state triplet or that the singlet–triplet gap is less than 0.2 kcal/mol.

In theoretical studies of TME and other diradicals, it has been standard practice to optimize the geometry of the triplet (T) state by means of the restricted open-shell (ROHF) or unrestricted (UHF) Hartree–Fock methods and either to employ this geometry also for the singlet (S) state or to optimize the geometry of the singlet state by means of the two-configurational SCF (TCSCF) procedure. (A wave function with a minimum of two Slater determinants is required to describe the singlet diradical.[4]) Although, it has been noted that the UHF and TCSCF procedures may prove inadequate for describing the geometries of diradicals,[5] electron correlation effects have generally been included at the Hartree–Fock or TCSCF optimized geometries (see, for example, ref 6). It is possible that geometry optimizations carried out using the multiconfigurational self-consistent field (MCSCF) method could lead to significantly different geometries, which, in turn, could cause an appreciable change in the singlet–triplet gap. In this paper we present the results of MCSCF calculations on the lowest singlet and triplet states of TME. Geometry optimizations were carried out with different choices of active orbital spaces and configuration lists in order to gain a more detailed understanding of the importance of electron correlation effects on the geometries and on the singlet–triplet gap.

II. Computational Methodology

The geometries were optimized for structures of D_{2h}, D_{2d}, and D_2 symmetry. Two different active orbital spaces were used in the geometry optimizations carried out using the MSCSF method. The smaller of these has two active electrons in two active orbitals, the HOMO and LUMO, and the larger has six active electrons in six active orbitals, the six valence π and π^* orbitals. Hereafter, these two procedures are referred to as MCSCF(2,2) and MCSCF(6,6), where the first number refers to the number of active electrons and the second to the number of active orbitals. For the singlet state, the MCSCF(2,2) and TCSCF procedures are equivalent, while for the triplet state, the MCSCF(2,2) and ROHF procedures are equivalent. The geometry of the triplet state was also optimized in the UHF approximation.

The MCSCF(6,6) procedure includes all symmetry-allowed configurations in the six orbital active space. The geometry of the singlet state has also been optimized by means of the MCSCF(6,6)SD procedure,

(1) Borden, W. T.; Davidson, E. R. *J. Am. Chem. Soc.* **1977**, *99*, 4587.
(2) Du, P.; Borden, W. T. *J. Am. Chem. Soc.* **1987**, *109*, 930.
(3) Dowd, P. *J. Am. Chem. Soc.* **1970**, *92*, 1066. Dowd, P.; Chang, W.; Paik, Y. H. *J. Am. Chem. Soc.* **1986**, *108*, 7416.
(4) Borden, W. T. In *Diradicals*; Borden, W. T., Ed.; Wiley-Interscience: New York, 1982; pp 1–72.
(5) Borden, W. T.; Davidson, E. R.; Feller, D. *Tetrahedron* **1982**, *38*, 737. Lahti, P. M.; Rossi, A.; Berson, J. A. *J. Am. Chem. Soc.* **1985**, *107*, 4362.
(6) Du, P.; Hrovat, D. A.; Borden, W. T.; Lahti, P. M.; Rossi, A. R.; Berson, J. A. *J. Am. Chem. Soc.* **1986**, *108*, 5072.

0002-7863/92/1514-4743$03.00/0